ORIGINAL ARTICLE

Diffusion-weighted MRI in the characterization of pleural effusions

Nagihan İnan, Arzu Arslan, Gür Akansel, Zeliha Arslan, Levent Eleman, Ali Demirci

PURPOSE
To evaluate the value of diffusion-weighted imaging (DWI) in the differential diagnosis of pleural effusions.

MATERIALS AND METHODS
58 pleural effusions (21 transudative, 37 exudative) were included in this prospective study. Single-shot echo-planar spin echo DWI was performed with two b factors (500 and 1000 s/mm^2), and apparent diffusion coefficients (ADCs) were calculated. On diffusion-weighted (DW) trace images, signal intensity (SI) of the pleural effusions was visually compared to the SI of the paraspinal muscles with the use of a 3-point scale: 0: isointense, 1: moderately hyperintense, 2: significantly hyperintense. For quantitative evaluation, effusion-to-paraspinal muscle SI ratios, and ADCs of the effusions were compared between the groups.

RESULTS
On visual evaluation, most of the transudative effusions were isointense, while most of the exudative effusions were hyperintense on DWI with b factors of 500 and 1000 s/mm^2. Quantitatively, with a b factor of 500 and 1000 s/mm^2, effusion-to-paraspinal muscle SI ratios of the exudative effusions were significantly higher than those of transudative effusions. The ADCs of the exudative effusions were significantly lower than those of transudative effusions (mean ADC was $3.3 \times 10^{-3} \pm 0.7$ mm^2/s for exudative effusions, and $3.7 \times 10^{-3} \pm 0.3$ mm^2/s for transudative effusions). Setting the cut-off value at 3.6×10^{-3}, ADC had a sensitivity of 71% and a specificity of 63% for differentiating transudative from exudative effusions.

CONCLUSION
DWI may help in the differential diagnosis of pleural effusions.

Key words: • diffusion magnetic resonance imaging • pleural effusion

From the Departments of Radiology (N.İ. ✉ inannagihan@ekolay.net, A.A., G.A., A.D.), Pulmonary Diseases (Z.A.), and Pediatric Surgery (L.E.), Kocaeli University School of Medicine, Kocaeli, Turkey.

Pleural effusion detected in a patient requires careful differential diagnosis, as the therapy depends on the nature of fluid. Diagnosis is made on the basis of clinical, biochemical, and pathological findings. Biochemical analysis of the fluid obtained by thoracentesis is usually the first step in distinguishing exudative effusions (EEs) from transudative effusions (TEs) (1). The Light criteria evaluating protein and lactate dehydrogenase (LDH) concentration in blood and pleural effusion can be used to differentiate EEs from TEs (2). However, occasionally Light criteria may misclassify a TE as an EE, especially in patients who have undergone diuresis (3, 4). In such cases, albumin levels in blood and pleural fluid help in the differentiation (3, 4). If the fluid is definitively identified as EE, additional testing (such us pleural fluid cytology, Gram staining, and culture) is necessary to evaluate local factors (5). If cytology is negative, biopsy of the pleura may be performed (5, 6). A noninvasive imaging method in the diagnosis of such cases may avoid risks associated with unnecessary pleural biopsies.

Hounsfield unit (HU) measurements in computed tomography (CT) (7) and conventional magnetic resonance imaging (MRI) based on precontrast signal intensity (SI) values in T1-weighted (T1W) and T2-weighted (T2W) images as well as post-gadolinium T1W images with fat saturation (8–10), have been used in the differential diagnosis of EE and TE. Results, however, were not reliable.

DWI is based on the restriction of random translational molecular motion (Brownian motion) of water, determined by the diffusion coefficient. It has been mainly used in the brain, especially for the diagnosis of acute cerebral infarction (11) and characterization of epidermoid and arachnoid cysts (12). Recently, it has also been used to characterize various cystic or solid lesions of abdominal organs (13–15). In this study, we evaluated the contribution of DWI in the differentiation of pleural effusions.

Materials and methods

Patients

Fifty-eight pleural effusions in 58 consecutive patients (27 females, 31 males), detected with any radiological modality between March and December 2007 were included in this prospective study. Causes of the EEs (37 patients; 17 females, 20 males) were: pneumonia (6 patients), tuberculosis (2 patients), malignancy (20 patients), chylothorax (4 patients), pulmonary embolism (1 patient), and intraabdominal abscess (4 patients). For the TEs (21 patients; 10 females, 11 males) the causes were: congestive heart failure (18 patients), chronic renal insufficiency (2 patients) and superior vena cava obstruction (1 patient). Primary malignancies detected in 20 patients were as follows: 12 patients had lung cancer, 3 patients had lymphoma, 1 patient had an ovarian tumor, 2

patients had mesothelioma, and 2 patients had liver tumor. Thirty-two patients had bilateral effusions (18 with congestive heart failure, 2 with chronic renal insufficiency, 1 with superior vena cava obstruction, 4 with intraabdominal abscesses, 3 with malignancy, and 4 with chylothorax). Of these bilateral effusions, only the side of the fluid sampling was evaluated on DWI. The mean age was 50.3 years (range, 2–78 years) and 49.3 years (range, 4–94 years) in the EE and the TE groups, respectively.

All cases underwent ultrasonography (US) examinations in order to evaluate the presence of an adequate amount of effusion. Due to limited resolution of the DWI, effusions thinner than 1 cm were not included. In addition, claustrophobic and severe dyspneic patients were excluded from the study. The nature of all effusions was confirmed by thoracentesis after MRI. Light criteria (2), and/or pleural fluid-to-serum albumin or protein gradient (4) were used to establish the exudative or transudative nature of pleural effusions. The diagnosis of tuberculous effusions was confirmed by positive pleural culture or biopsy. Pleural fluid was considered a parapneumonic effusion if the patient had typical clinical (acute febrile episode, purulent sputum), laboratory, and radiologic findings of pulmonary infection. The diagnosis of the malignant effusion was confirmed by positive pleural cytology and biopsy. All effusions were considered TEs if the patient had typical clinical (peripheral edema, orthopnea, paroxysmal nocturnal dyspnea) and radiologic findings (cardiomegaly, lung congestion) of congestive heart failure or chronic renal failure.

The study was approved by the institutional review board and protocol review committee. Since the tests employed were part of the routine clinical evaluation of these patients, informed consent was not required by the review board. We obtained blanket consent from all patients for the use of their findings for research and educational purposes, with patient privacy secured.

MR imaging

All patients were examined with a 1.5 Tesla MR scanner (Gyroscan Intera; Philips Medical Systems, Eindhoven, The Netherlands) using a four-element phased-array body coil. This system has a maximal gradient strength of 30 mT/m and a slew rate of 150 mT/m/ms. All patients were examined initially with precontrast axial T1W breath-hold spoiled gradient echo (fast field echo, FFE) with and without fat suppression (TR/TE/FA/NEX, 169/4.6/80/1), coronal and axial T2W single shot turbo spin echo (SS-TSE) (TR/TE/NEX/TSE factor, 700/80/1/72), and axial T2W SS-TSE with fat suppression (TR/TE/NEX/TSE factor, 700/80/1/72). Subsequently, 3 series of axial single-shot spin-echo echo-planar (SS-SE-EP) DW images (TR/TE/NEX/echo-planar imaging factor, 1000/81/1/77; sensitizing gradients in x, y, z directions) were acquired using the following b values: 0, 500, and 1000 s/mm^2. ADC maps were reconstructed from these images. Fat suppression was performed by using spectral saturation inversion recovery (SPIR) technique. MRI, including DWI, consisted of a multisection acquisition with a slice thickness of 6 mm, an intersection gap of 1 mm, and an acquisition matrix of 128 × 256. The field of view varied between 455 and 500 mm. All sequences were acquired using a partially parallel imaging acquisition and SENSE (sensitivity encoding for fast MRI) reconstruction with a reduction factor (R) of 2. The scan time of the acquisition of each DWI series during a single breath-hold was 25 seconds.

Image analysis

1. Qualitative analysis:
   The SI of the pleural effusions in all three sets of DWI with b factors of 500, and 1000 s/mm^2 was visually assessed compared to the SI of the paraspinal muscles with the use of a 3-point scale as follows: 0, isointense; 1, moderately hyperintense; 2, significantly hyperintense. All images were independently assessed by two radiologists (N.I., A.A.) who were blinded to the clinical history and results of prior imaging studies. Results of the interpretations were compared. In three cases for which the results differed, the final score was reached by consensus after discussion.
2. Quantitative analysis:
   Quantitative analysis was made using a dedicated work station (Dell Workstation Precision 650, View Forum release 3.4-inch system). SIs of the pleural effusion and paraspinal muscle were measured by one radiologist (N.I.) for each b factor (500 and 1000 s/mm^2) using a region of interest (ROI) of the same size. The ROI was placed centrally and the size of the ROI was kept as large as possible, yet avoiding interference from the surrounding tissue. In addition, the ADC maps were created automatically and the mean ADC values of pleural effusions were determined on images with b factors 0 and 1000 s/mm^2. To avoid possible magnetic susceptibility artifact, SI measurements and ADC values were calculated far from the lung-fluid interfaces and diaphragmatic regions. The average of the three measurements was recorded as the final SI or ADC.

Statistical analysis

For qualitative analysis, Fisher exact test was used to assess the differences between the groups. For the quantitative evaluation, effusion-to-paraspinal muscle SI ratios (SIRs), and ADCs of the EEs and TEs were compared. The fitness of numeric data set to normal distribution was determined by Kolmogorov-Smirnov test. The data were normally distributed. Student's t test was used to assess the differences between EEs and TEs in terms of SIRs and ADCs. For the subgroups of EEs, the data were not normally distributed; hence the differences between subgroups were analyzed by Kruskal-Wallis test. A P value < 0.05 was considered statistically significant. To evaluate the diagnostic performance of the quantitative tests (SIRs, and ADC) for the differentiation of pleural effusions and to describe the sensitivity and specificity of the tests, receiver operating characteristic (ROC) analysis was performed. The areas and standard errors for each ROC curve were calculated by the method described by Metz (16). The area under the ROC curve reflects the performance of the tests. The optimum cut-off point was determined as the value that best discriminates between the two groups in terms of maximum sensitivity and minimum number of false-positive results. All statistical analyses were performed using SPSS (Statistical Package for the Social Sciences, Chicago, USA) software.
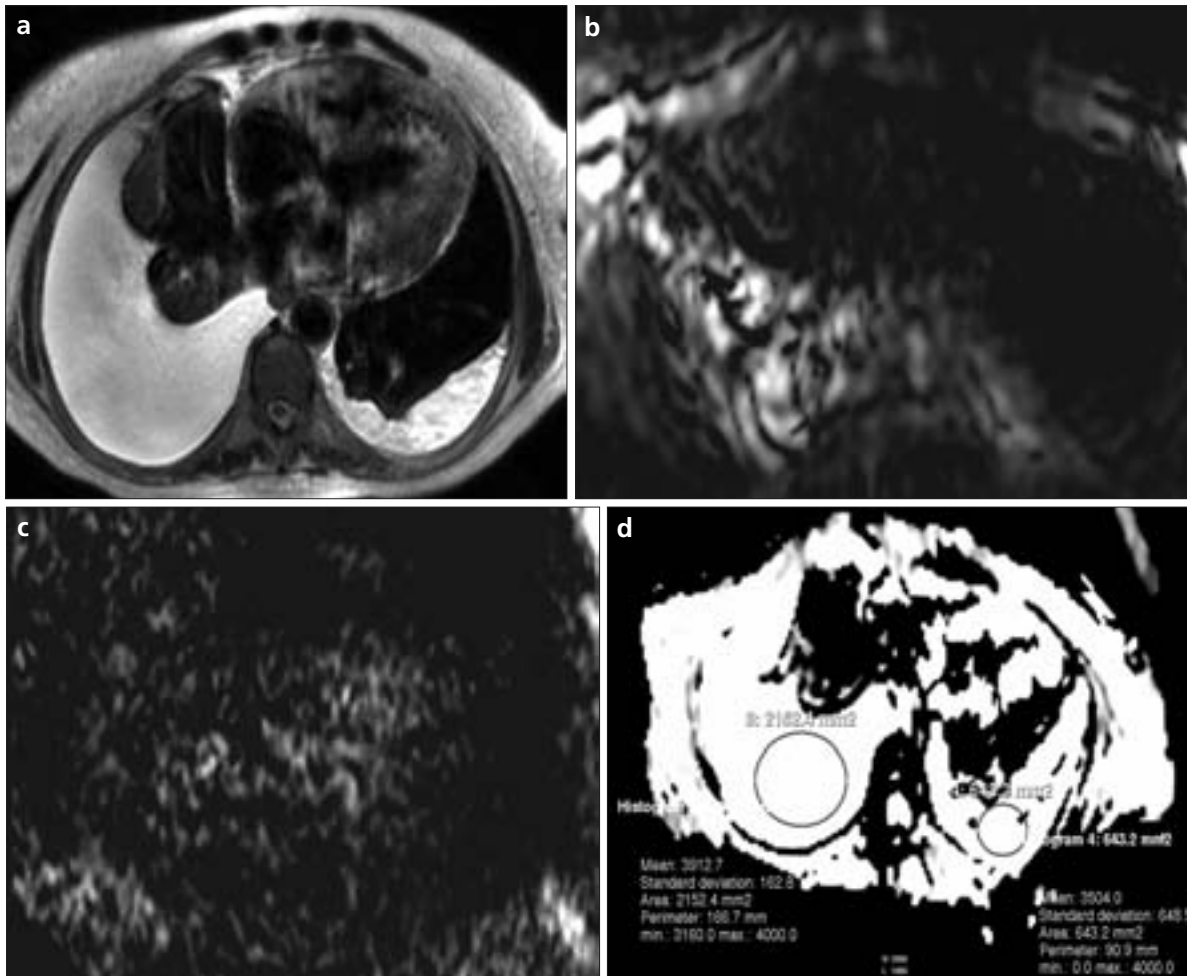
Figure 1. a–d. A 70-year-old female with chronic renal failure. Axial T2-weighted turbo spin-echo MR image **(a)** shows bilateral pleural effusions. These effusions appear hyperintense on the diffusion-weighted image with b factor 500 s/mm^2 **(b)** and isointense on the diffusion-weighted image with b factor 1000 s/mm^2 **(c)**. Apparent diffusion coefficient (ADC) map **(d)**. (ADC, 3.9×10^{-3} on the right, and 3.5×10^{-3} mm^2/s on the left-sided effusions).

Results

Qualitative analysis

Results of the visual evaluation of the SI of the effusions in diffusion trace images with a b factor of 500 and 1000 s/mm^2 are shown in Table 1. On these images, the SIs of EEs were significantly higher than those of TEs ($P < 0.001$ and $P = 0.04$). On images with a b factor of 500 and 1000 s/mm^2, most of the TEs were isointense (Fig. 1), while most of the EEs were hyperintense (Fig. 2).

Quantitative analysis

The maximum thickness of fluid collections ranged between 12–117 mm (mean thickness, 39.3 ± 26.9 mm) and 12–65 mm (mean thickness, 34.5 ± 18.8 mm) for EEs and TEs, respectively.

The results of the quantitative analysis of the DWI are shown in Table 2. With b factors of 500 and 1000 s/mm^2, the SIRs of the EEs were significantly higher than those of the TEs. The area under the ROC curve was 0.604 ± 0.114 for SIR on DWI with a b factor 500 s/mm^2. Setting the cut-off value at 0.7, SIR had a sensitivity of 64% and a specificity of 67% for differentiating TEs from EEs. The positive predictive value, negative predictive value, and accuracy of SIR were determined as

Table 1. Visual evaluation of the signal intensities of transudative effusions and exudative effusions on diffusion weighted MR images with b factors of 500 and 1000 s/mm^2

	MR signal intensity	TEs (n = 21)	EEs (n = 37)
b = 500 s/mm^2	Significantly hyperintense	–	21 (57%)
	Moderately hyperintense	10 (48%)	13 (35%)
	Isointense	11 (52%)	3 (8%)
b = 1000 s/mm^2	Significantly hyperintense	–	13 (35%)
	Moderately hyperintense	6 (29%)	18 (49%)
	Isointense	15 (71%)	6 (16%)

TEs, transudative effusions; EEs, exudative effusions
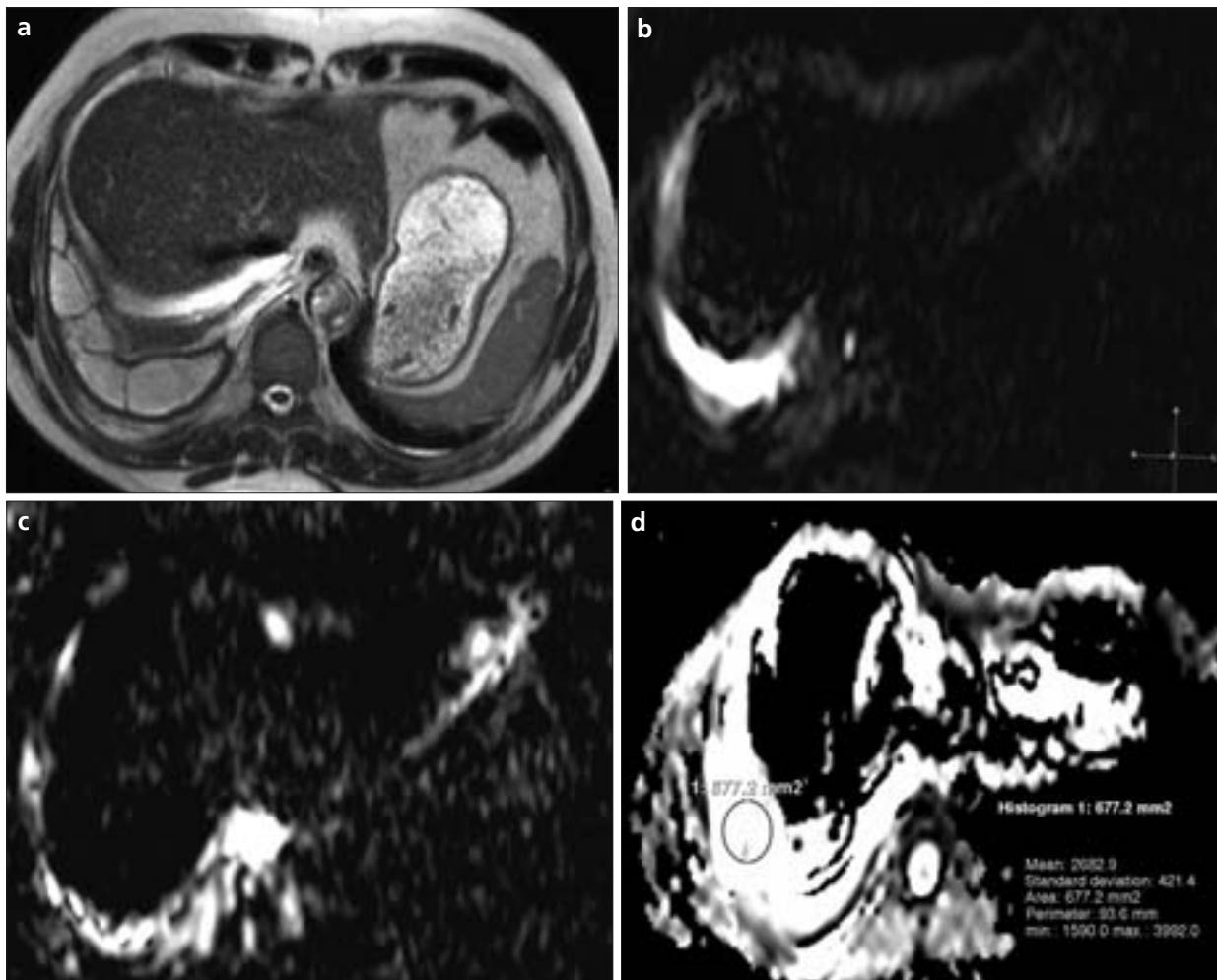
Figure 2. a–d. A 62-year-old male with empyema. Axial T2-weighted turbo spin-echo MR image **(a)** shows right-sided empyema. This effusion appear hyperintense on the diffusion-weighted image with a b factor 500 **(b)**, and 1000 s/mm^2 **(c)**. Apparent diffusion coefficient (ADC) map **(d)** (ADC, 2.6×10^{-3} mm^2/s).

66%, 65%, and 66%, respectively. The area under the ROC curve was 0.643 ± 0.110 for SIR on DWI with a b factor 1000 s/mm^2. We could not obtain a sufficiently discriminative cut-off value by the ROC analysis for differentiating TEs from EEs. The ADCs of EEs were significantly lower than those of the TEs. The area under the ROC curve was 0.694 ± 0.083 for ADC. With a cut-off value of 3.6×10^{-3}, ADC had a sensitivity of 71% and a specificity of 63% for differentiating TEs from EEs. The positive predictive value, negative predictive value, and accuracy of ADC values were determined as 66%, 68%, 67%, respectively (Fig. 3). When the subgroup analysis was done, we could not obtain statistical significance in SIRs or ADCs between subgroups.

Discussion

A variety of imaging techniques can be used to evaluate the pleura and the pleural space (17, 18). US allows easy identification of pleural fluid and loculation and differentiation from pleural masses (17). Pleural thickening or nodularity on CT or MRI is suggestive of pleural metastases, but these findings may also be seen with benign effusions (18). CT in characterizing pleural fluid based on attenuation values has been recently used in differentiation of pleural effusions (7). According to this study, although the mean attenuation of EEs was significantly higher than TEs (with the strongest relationship with protein content), the clinical use of CT numbers to characterize pleural fluid is not

Table 2. Quantitative analysis of diffusion weighted imaging of transudative effusions and exudative effusions (b = 500 and 1000 s/mm^2)

	TEs (n = 21)	EEs (n = 37)	P
b = 500 s/mm^2 SIR	0.6 ± 0.3	1.3 ±1.2	0.045
b = 1000 s/mm^2 SIR	1.0 ±0.5	1.6 ±1.1	0.009
ADC (×10^{-3} mm^2/s)	3.7 ± 0.3	3.3 ± 0.7	0.004

Data are mean ± SD. SIR, signal intensity ratio; ADC, apparent diffusion coefficient; TEs, transudative effusions; EEs, exudative effusions
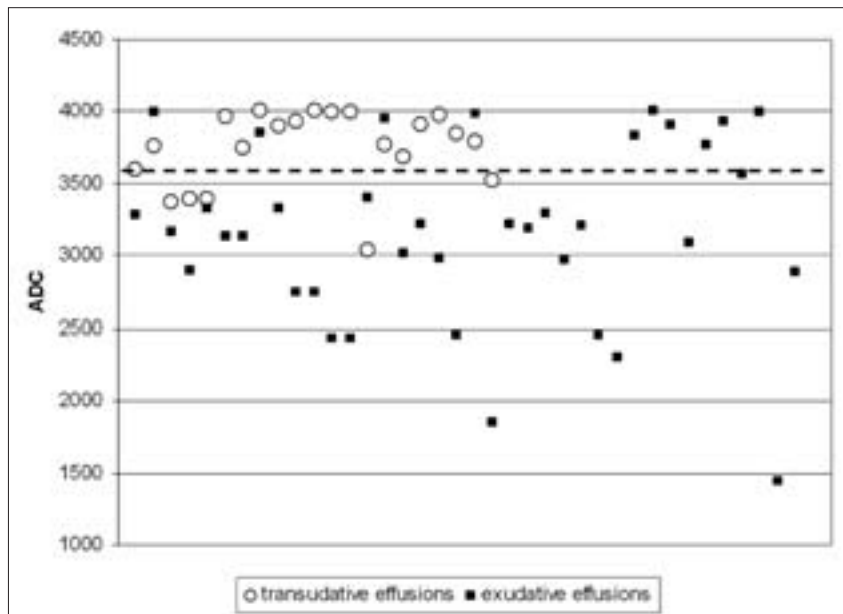
Figure 3. Scattergram distribution of apparent diffusion coefficients (ADCs) of transudative and exudative effusions.

recommended, as their accuracy was only moderate. Moreover, there was a notable overlap in attenuation values between TE and EEs. A study by Shiono et al. (19) showed that on T1W and T2W MRI, SI of effusions depended mainly on the concentration of protein, whereas on gradient echo images it depended mainly on the concentration of blood. Hence, MR examination could be useful in differentiating an EE or a hemorrhagic effusion from a serous effusion. However, the values of two groups overlapped, so that differentiation based on only SI was usually insufficient (8, 9). In a previous study, the contrast enhancement patterns of effusions on late phase (20 minutes after contrast administration) on fat suppressed T1W images have been defined (10). According to this study, EEs displayed significant enhancement. Although suggestive, this examination was not practical because of long examination times.

The use of DWI in the thorax is hindered by limitations such as physiologic motion artifact caused by respiration and cardiac motion. The effects of respiration and cardiac motion can be reduced by using breath-hold and pulse-triggered sequences. Due to the rapid acquisition capabilities and high signal-to-noise ratio, the best image quality has been obtained with breath-hold SS-SE-EPI sequences (20–22). Parallel imaging is crucial to reduce the distortion of SS-SE-EPI DWI (21). In our study, DW imaging was obtained using a breath-hold EPI sequence, which allowed short echo time, SPIR fat suppression pulse, and SENSE.

Over the past few years, several studies have demonstrated that DWI is helpful in differentiation of various cystic lesions (12–15). Hakyemez et al. (12) reported that the low ADCs of epidermoid cysts (mean ADC was $1.15 \pm 0.17 \times 10^{-3}$ mm^2/s for epidermoid cysts, and $3.41 \pm 0.17 \times 10^{-3}$ mm^2/s for arachnoid cysts) were the result of the dense keratinaceous content of the cysts, which limits the diffusivity of protons. There are only few reports on the use of DWI in the cystic lesions of the liver. Chan et al. (13) have suggested that the ADC values are lower in hepatic abscess cavities ($0.67 \pm 0.35 \times 10^{-3}$ mm^2/s) than in the necrotic portions of tumors ($2.65 \pm 0.49 \times 10^{-3}$ mm^2/s), depending on the viscosity of the lesions. Similarly, Inan et al. (14) suggested that the ADCs were lower in hepatic hydatid cysts ($3 \pm 0.6 \times 10^{-3}$ mm^2/s) than in simple cysts ($3.5 \pm 0.5 \times 10^{-3}$ mm^2/s). Since the hydatid cyst contains viscous hydatid sand, the ADC of the hydatid cyst is decreased. In addition, Nakayama et al. (15) reported that the ADCs were lower in mature cystic teratomas than in endometrial cysts as well as other benign and malignant ovarian cystic neoplasms. According to this study, the low ADCs of the mature cystic teratomas were attributed to the keratinoid substance within the tumors.

To our knowledge, the role of DWI in the differential diagnosis of pleural effusions has been reported in a previous study of 52 patients, in which EE displayed lower ADC values than TE ($3.18 \times 10^{-3} \pm 1.82$ and $3.42 \times 10^{-3} \pm 0.76$, respectively) (23). This study was based only on ADC values of effusions, without any quantitative and qualitative analysis of DW trace images. In our study, we evaluated both DW trace images (b factors of 500 and 1000) and ADC maps quantitatively and qualitatively.

In our study, significant differences between the SIs of pleural effusions were found on images with b factors of 500 and 1000 s/mm^2. SIs of EEs were higher than TEs with b factors of both 500 and 1000 s/mm^2. Magnetic susceptibility effects resulting in geometric distortion artifact are more severe with higher b values. For that reason, in our study, DW images with b factor of 500 s/mm^2 were more useful than images with b factor of 1000 s/mm^2 for evaluation of SIs. However, DW images with b factor of 1000 s/mm^2 are optimal to obtain SIs because the signal of the DW image contains contributions from the spin density as well as T1 and T2 relaxation times. Therefore, fluids may display a strong T2 effect (T2 shine-through effect) instead of reduced diffusion, especially with lower b factors. Diffusion can be quantitatively evaluated by ADC, which is free of the T2 shine-through effect (11, 24). In our series, the mean ADC of the EEs was significantly lower than that of the TEs. Therefore, the hyperintensity of EEs on DW trace images cannot be totally attributed to the T2 shine-through effect. Differences between the ADCs can be caused by the differences in fluid contents. Since parapneumonic effusions, malignant effusions, and tuberculous pleuritis have proteinaceous fluid and rich cell counts (inflammatory cells, tumor cells, and lymphocytes, respectively), and chylothorax has high lipid levels (cholesterol crystals or lecithin-globulin complexes), these fluid collections have a decreased ADC. Conversely, TEs have lower viscosity and thus higher ADC (5).

DWI may lose accuracy in patients receiving diuretics and patients with hypoalbuminemia. In patients receiving

diuretics, false exudative effusions on DWI can be explained by the relative increase in the pleural concentrations of protein leading to decrease in diffusion. In patients with hypoalbuminemia, false transudative effusion can be explained by the relative decrease in the pleural concentrations of protein (23).

This study has technical limitations. The main limitation was that the EPI sequence employed with a higher b value had a lower SNR, resulting in greater image distortion. In addition, the EPI sequence causes anatomic distortion due to susceptibility effects (21). We did not utilize pulse triggered DWI. Mürtz et al. (20) evaluated 12 patients using an SS-SE-EPI sequence with ECG triggering to minimize the influence of cardiac pulsation. They found that DWI without pulse-triggering reduces the accuracy of measurements of ADCs in abdominal organs. For this reason, accuracy of ADCs in pleural fluids can be improved by using pulse-triggering technique.

In conclusion, diagnosis of pleural effusions is usually possible with the combined use of specific morphologic features on imaging (thickening or nodularity of pleura, internal structure, the enhancement pattern, or calcification), laboratory evaluation, and clinical information. However, occasionally the differentiation of EEs from TEs may still be difficult. Our preliminary data suggest that DWI may be helpful in this setting. Despite fair sensitivity and specificity, this sequence can easily be added to routine thorax MRI protocol because of very short examination time. Hence, DW images give clues to the radiologist for interpretation of pleural effusions in daily practice. Our findings need further studies for confirmation; likewise, statistical differences of ADCs among fluid types should be studied in larger series.

References

1. Romero-Candeira S, Hernández L, Romero-Brufao S, Orts D, Fernández C, Martín C. Is it meaningful to use biochemical parameters to discriminate between transudative and exudative pleural effusions? Chest 2002; 122:1524–1529.
2. Light RW, MacGregor MI, Luchsinger PC, Ball WC. Pleural effusions: the diagnostic separation of transudates and exudates. Ann Intern Med 1972; 77:507–513.
3. Eid AA, Keddissi JI, Samaha M, Tawk MM, Kimmell K, Kinasewitz GT. Exudative effusions in congestive heart failure. Chest 2002; 122:1518–1523.
4. Romero-Candeira S, Fernandez C, Martin C, Sánchez-Paya J, Hernández L. Influence of diuretics on the concentration of proteins and other components of pleural transudates in patients with heart failure. Am J Med 2001; 110:681–686.
5. Tarn AC, Lapworth R. BTS guidelines for investigation of unilateral pleural effusion in adults. Thorax 2004; 59:358–359.
6. Erasmus JJ, McAdams HP, Rossi SE, Goodman PC, Coleman RE, Patz EF. FDG PET of pleural effusions in patients with non-small cell lung cancer. AJR Am J Radiol 2000; 175:245–249.
7. Nandalur KR, Hardie AH, Bollampally SR, Parmar JP, Hagspiel KD. Accuracy of computed tomography attenuation values in the characterization of pleural fluid: an ROC study. Acad Radiol 2005; 12:987–991.
8. Davis SD, Henschke CI, Yankelevitz DF, Cahill PT, Yi Y. MR imaging of pleural effusions. J Comput Assist Tomogr 1990; 14:192–198.
9. Tscholakoff D, Sechtem U, de Geer G, Schmidt H, Higgins CB. Evaluation of pleural and pericardial effusions by magnetic resonance imaging. Eur J Radiol 1987; 7:169–174.
10. Frola C, Cantoni S, Turtulici I, et al. Transudative vs exudative pleural effusions: differentiation using Gd-DTPA-enhanced MRI. Eur Radiol 1997; 7:860–864.
11. Ozsunar Y, Sorensen AG. Diffusion- and perfusion-weighted magnetic resonance imaging in human acute ischemic stroke: technical considerations. Top Magn Reson Imaging 2000; 11:259–272.
12. Hakyemez B, Yildiz H, Ergin N, Uysal S, Parlak M. FLAIR and diffusion weighted MR imaging in differentiating epidermoid cysts from arachnoid cysts. Tani Girisim Radyol 2003; 9:418–426.
13. Chan JH, Tsui EY, Luk SH, et al. Diffusion-weighted MR imaging of the liver: distinguishing hepatic abscess from cystic or necrotic tumor. Abdom Imaging 2000; 26:161–165.
14. Inan N, Arslan A, Akansel G, et al. Diffusion-weighted imaging in the differential diagnosis of simple and hydatid cysts of the liver. AJR Am J Radiol 2007; 189:1031–1036.
15. Nakayama T, Yoshimitsu K, Irie H, et al. Diffusion-weighted echo-planar MR imaging and ADC mapping in the differential diagnosis of ovarian cystic masses: usefulness of detecting keratinoid substances in mature cystic teratomas. J Magn Reson Imaging 2005; 22:271–278.
16. Metz CE. ROC methodology in radiologic imaging. Invest Radiol 1986; 21:720–733.
17. McLoud TC, Flower CD. Imaging the pleura: sonography, CT, and MR imaging. AJR Am J Radiol 1991; 156:1145–1153.
18. Quint LE, Francis IR, Wahl RL, Gross BH, Glazer GM. Preoperative staging of non-small-cell carcinoma of the lung: imaging methods. AJR Am J Radiol 1995; 164:1349–1359.
19. Shiono T, Yoshikawa K, Takenaka E, Hisamatsu K. MR imaging of pleural and peritoneal effusion. Radiat Med 1993; 11:123–126.
20. Mürtz P, Flacke S, Traber F, van den Brink JS, Gieseke J, Schild HH. Abdomen: diffusion-weighted MR imaging with pulse-triggered single-shot sequences. Radiology 2002; 224:258–264.
21. Naganawa S, Kawai H, Fukatsu H, et al. Diffusion-weighted imaging of the liver: technical challenges and prospects for the future. Magn Reson Med Sci 2005; 4:175–186.
22. Chow LC, Bammer R, Moseley ME, Sommer FG. Single breath-hold diffusion-weighted imaging of the abdomen. J Magn Reson Imaging 2003; 18:377–382.
23. Baysal T, Bulut T, Gökirmak M, Kalkan S, Dusak A, Dogan M. Diffusion-weighted MR imaging of pleural fluid: differentiation of transudative vs exudative pleural effusions. Eur Radiol 2004; 14:890–896.
24. Hakyemez B, Aksoy U, Yildiz H, Ergin N. Intracranial epidermoid cysts: diffusion-weighted, FLAIR and conventional MR findings. Eur J Radiol 2005; 54:214–220.